Supporting Information

Enhancing Catalytic Aerobic Oxidation Performance of Cyclohexane via Size Regulation of Mixed-Valence {V_{16}} Clusters-Based Metal-Organic Framework

Shuang Wang[†], Zhixia Sun[†], Xinyu Zou[†], Zhijuan Zhang[†], Guoyuan Fu[†], Lei Li[†], Xue Zhang[†], Fang Luo[†,]*

[†]*Key Laboratory of Polyoxometalate Science of the Ministry of Education, College of Chemistry, Northeast Normal University, Jilin 130024, P. R. China.*

The nucleation and growth equations are expressed as the following:

$$\frac{dN}{dt} = \beta exp[-\frac{A}{ln^2 S}] \quad \text{(S1)}$$

$$A=\frac{16\pi б^3 г^2}{3(\kappa T)^3};\ s=\frac{C}{C_{eq}}a \quad \text{(S2)}$$

β: Pre-finger factor

A: Parameters related to solid-liquid interface energy

б: Solid-liquid interface energy

г : Compound molecular volume

к : Constant T: Temperature

S: Supersaturation

C: Actual concentration of compound

C_{eq}: Saturated concentration of compound

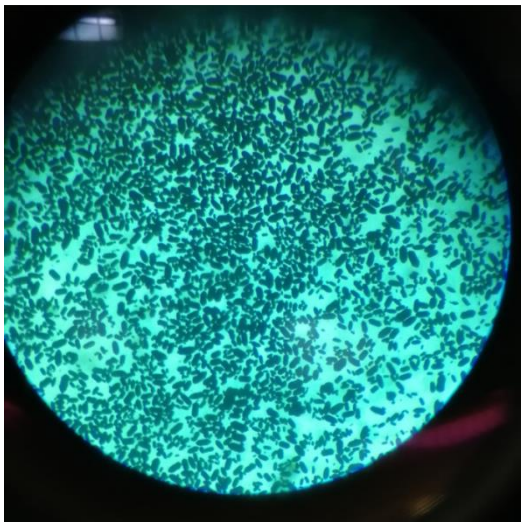

Fig.S1. The physical map of NENU-MV-1 grains with 2 mm.

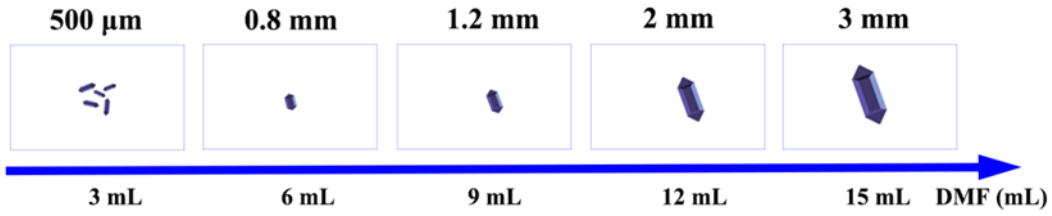

Fig. S2. Size evolution of NENU-MV-1 with increasing the volume of DMF.

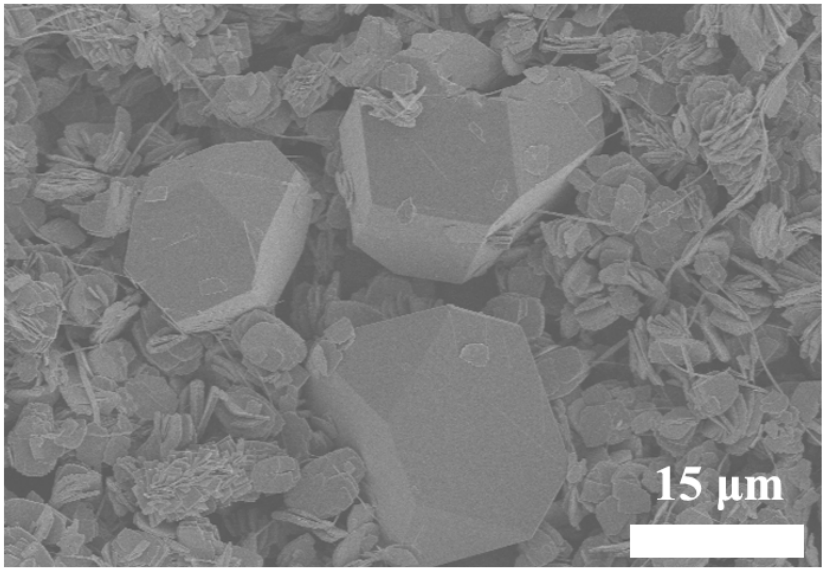

Fig. S3. The SEM images of NENU-MV-1 when the ratio of DMF to water is in the range of 2.5~4.

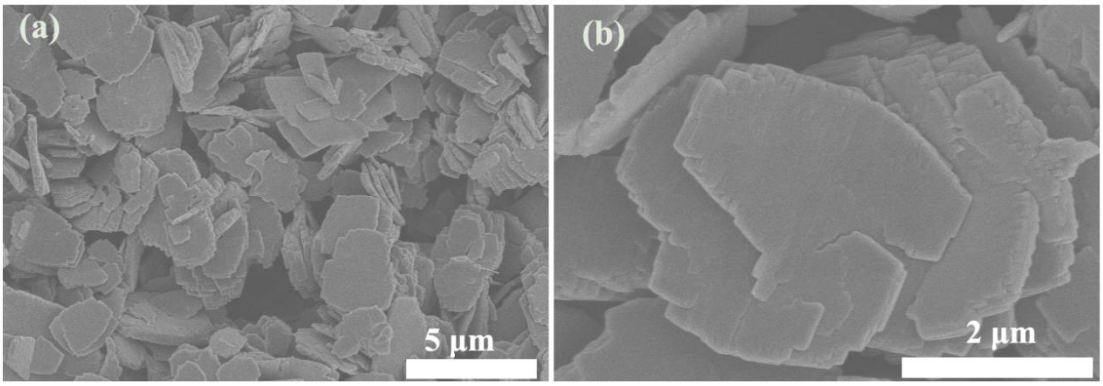

Fig. S4. (a). Wide range SEM images of dark green powders. (b). Small range SEM images of dark green powders.

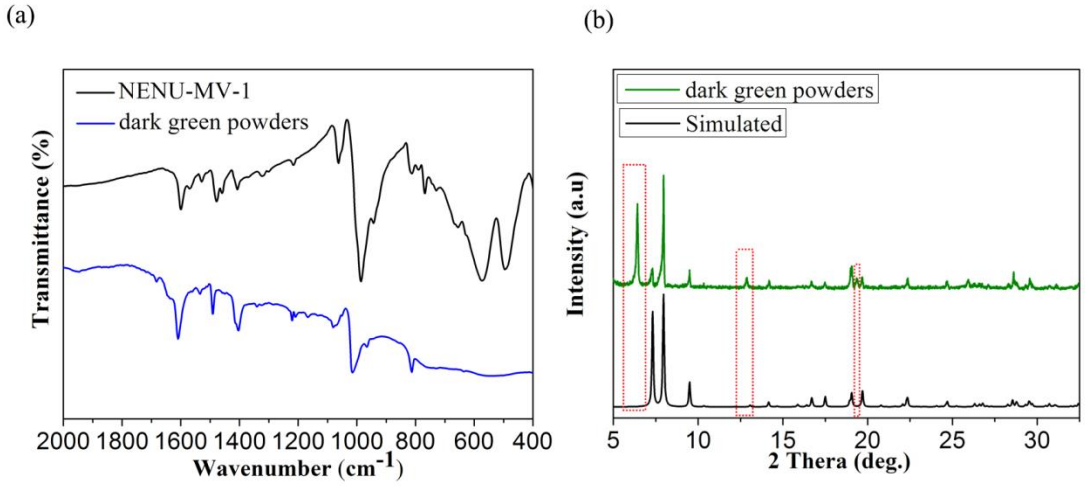

Fig. S5. (a). FT-IR measurements of dark green powders and NENU-MV-1. (b) The powder X-ray diffraction patterns of simulated and dark green powders.

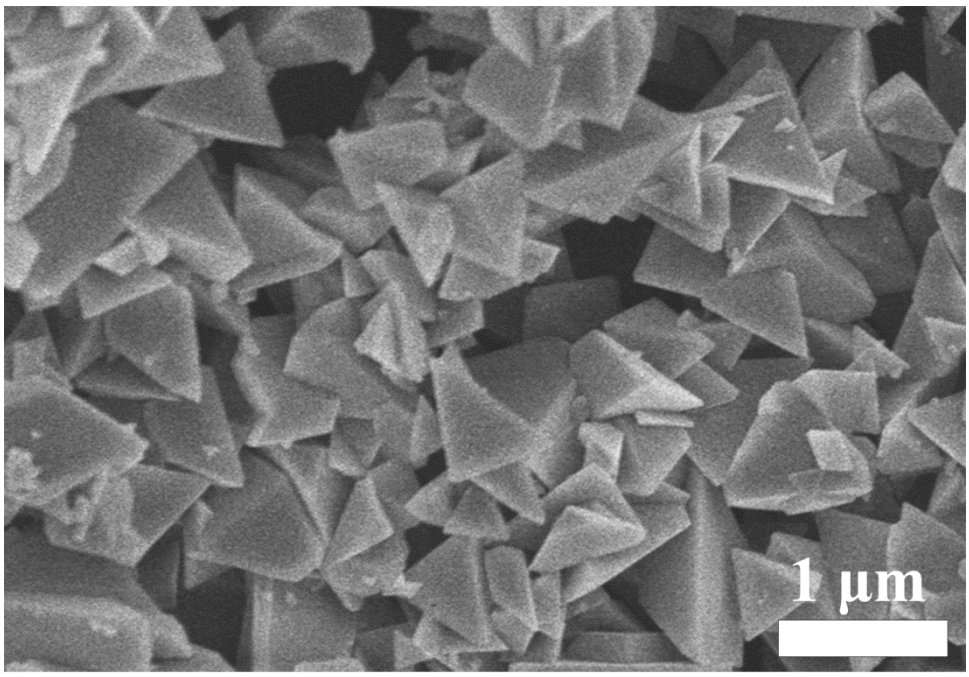

Fig. S6. The SEM images of NENU-MV-1 with 500 nm through increasing the molar ratio of ligand to nickel ions to 1.5.

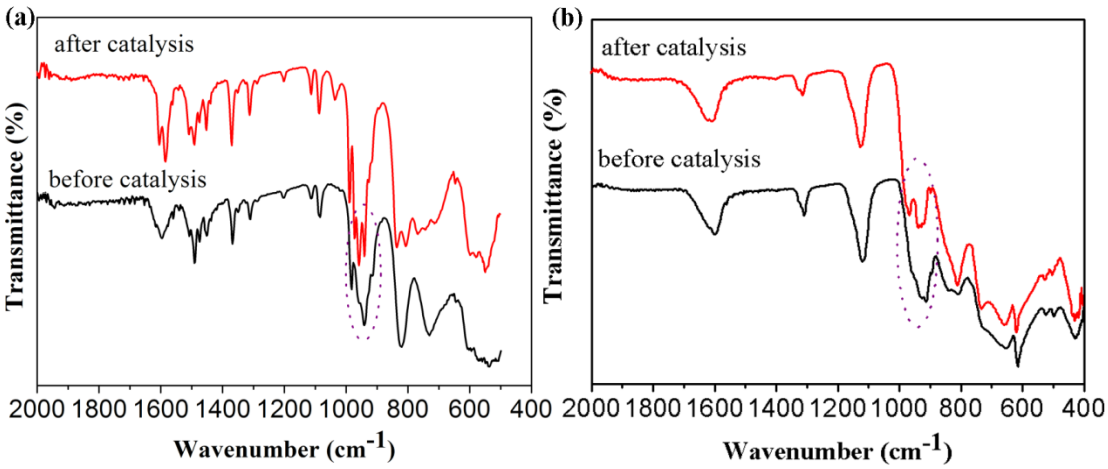

Fig. S7. (a) FT-IR measurements of $[C_8H_{17}N(CH_3)_3]_3H_3V_{10}O_{28}$ before and after catalysis, respectively. (b) FT-IR measurements of $K_{12}[V^{IV}_{18}O_{42}(H_2O)]\cdot 16H_2O$ before and after catalysis, respectively.

Table S1. Effect of Reaction Pressure with NENU-MV-1-500 nm

Entry	Reaction pressure (Mpa)	Conversion (%)	KA selectivity (%)	K/A (molar ratio)
1	1.0	24.6	99.9	0.63
2	1.2	26.8	82.7	0.72
3	1.5	30.1	74.6	0.80
4	1.8	32.2	68.1	0.87

Reaction conditions: cyclohexane (5 ml), NENU-MV-1-500 nm (50 mg), 150 ℃, 2 h, oxygen atmosphere.

Table S2. Effect of Reaction Temperature with NENU-MV-500 nm

Entry	Reaction temperature （℃）	Conversion （%）	KA selectivity (%)	K/A（molar ratio）
1	150	24.6	99.9	0.63
2	155	25.8	87.2	0.68
3	160	28.4	80.4	0.71
4	180	31.6	71.5	0.82

Reaction conditions: cyclohexane (5 ml), NENU-MV-1-500 nm (50 mg), 2 h, oxygen pressure (1 Mpa).

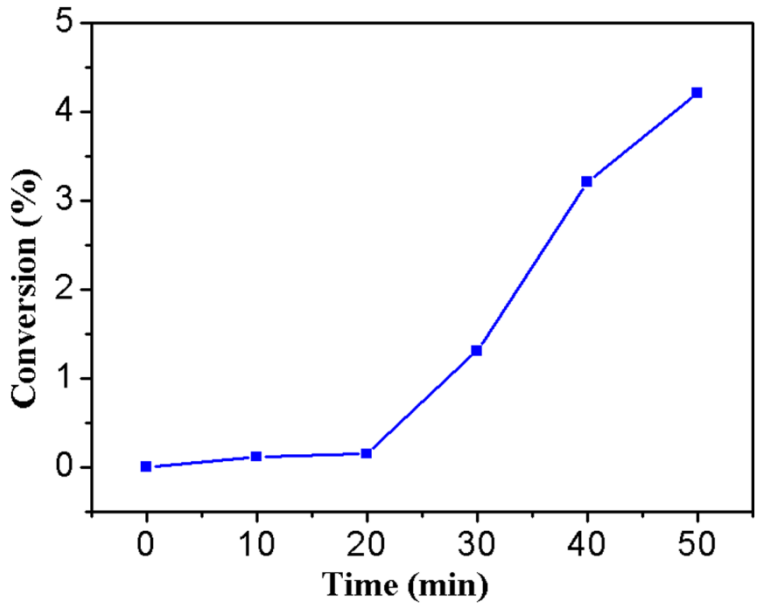

Fig. S8. Time course of the initial reaction rate of cyclohexane oxidation with NENU-MV-1-500 nm: cyclohexane (5 ml), catalyst (50 mg), O_2 (1 Mpa), 150 ℃, Time (1 h).

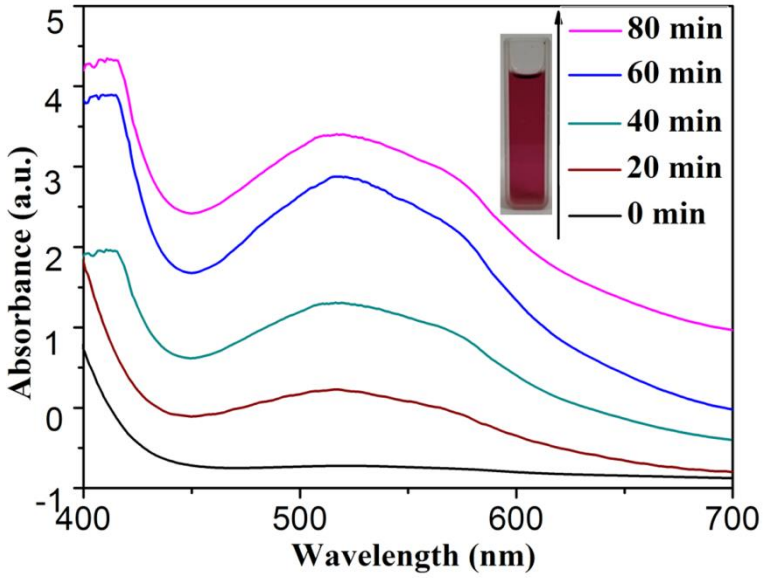

Fig. S9. UV-Vis adsorption spectrum of NBT with NENU-MV-1-500 nm as catalyst.

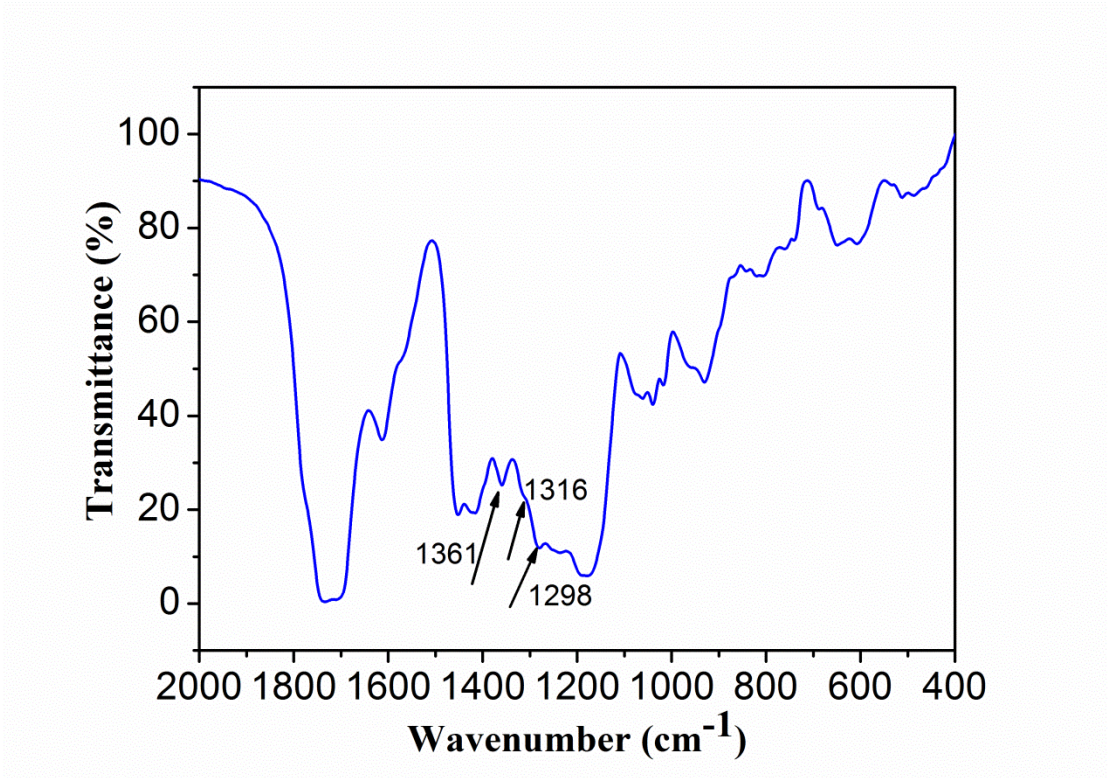

Fig. S10. FT-IR spectrum of the solution after 2 h of reaction of cyclohexane using NENU-MV-1-500 nm as the catalyst. The peaks at 1361, 1316, and 1298 cm^{-1} can be assigned to the vibrational modes of cyclohexyl hydroperoxide.

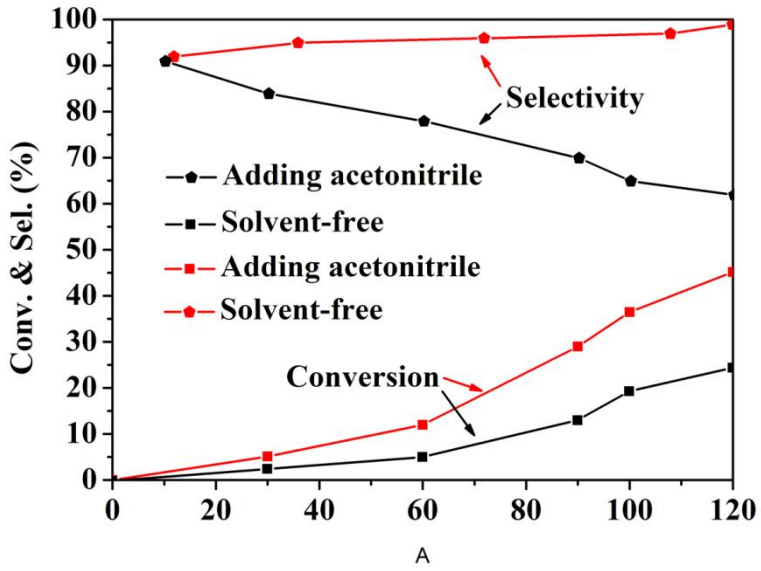

Fig. S11. Time course of the oxidation of cyclohexane with 10 atm O_2 catalyzed by

NENU-MV-1-500 nm under acetonitrile as a solvent and solvent-free conditions, respectively.

Table S3. Catalytic Performance of Different Catalysts for the Oxidation of Cyclohexane

Catalysts	Time (h)	Tem. (° C)	Pressure (Mpa)	Con. (%)	Sel. (%)	Publishing magazine
$Au_{75}Pd_{25}$ alloy icosahedrons	48	125	1.0	28.1	84.3	Nano Lett. 2015, 15, 2875-2880
$Au_{75}Pd_{25}$ alloy octahedrons	48	125	1.0	9.5	84.0	Nano Lett. 2015, 15, 2875-2880
Au−Pd/MIL-101	4	150	1.0	45.4	84.2	ACS Catal. 2013, 3, 647-654
CoD(p-Cl)PPCl/ZnO	2	155	1.0	6.23	89.4	Ind. Eng. Chem. Res. 2015, 54, 2425-2430
Cr-HMS	4	140	0.5	7.69	46.6	Ind. Eng. Chem. Res. 2010, 49, 5392–5399
V-HMS	4	140	0.5	9.34	92.4	
Ti-HMS	4	140	0.5	9.04	76.1	